Journal of Applied Electrochemistry **32**: 85–89, 2002.

Corrosion resistance of compositionally modulated Zn–Ni multilayers electrodeposited from dual baths

I. IVANOV, T. VALKOVA and I. KIRILOVA*
Institute of Physical Chemistry, Bulgarian Academy of Sciences, Sofia 1113, Bulgaria
*(*author for correspondence, e-mail: kirilova@ipchp.ipc.bas.bg)*

Received 14 August 2000; accepted in revised form 3 October 2001

Key words: corrosion resistance, modulated multilayers, nickel, zinc

Abstract

By successive deposition from dual baths containing Zn sulfate electrolyte and Ni sulfate–chloride electrolyte, smooth and bright compositionally modulated multilayered (CMM) coatings with different number, thickness and sequence of the sublayers were obtained. The corrosion resistance of the coatings was studied by anode potentiodynamic dissolution and by corrosion potential measurement. With increase in the number of sublayers, regardless of their individual thickness, the correlation between the quantity of Zn, dissolved at more negative potentials (between -1.250 and -0.750 V vs SSE), and the whole quantity of the metal in the coating, decreases. This correlation is smaller in CMM coatings ending with a Ni oversublayer compared to CMM coatings ending with a Zn oversublayer. The corrosion potentials of CMM coatings ending with a Zn oversublayer composed of a great number thin (0.7 μm) sublayers, are more positive (0.150/0.200 V) than the potentials of CMM coatings composed of a few thick (3.0 μm) sublayers. The most positive corrosion potentials (-0.750/-0.800 V vs SSE) have the CMM coatings ending with a Ni oversublayer; i.e. these multilayered coatings are the most corrosion resistant.

1. Introduction

Compositionally modulated multilayers (CMM) are coatings which consist of alternate sublayers of two or more components [1]. Such coatings have better corrosion resistance and physicomechanical properties than those observed in common alloys [1–13]. The production and investigation of the properties of CMM composed of Zn and Fe-group metals are of great interest but data concerning such CMM are very rare. Kalantary et al. [14] and Chawa et al. [15] deposited Zn–Ni CMM from pure Zn and Ni sulfate or sulfamate electrolytes and measured their corrosion resistance. A significant improvement in the corrosion characteristics of CMM is established relative to pure Zn coatings, this is because of the finer structure in each thin layer and the multiple layer effect. Electrochemical stripping methods have been proposed to characterize the alloy deposition process and product. Stripping studies are an accelerated corrosion test of the deposits [16–30]. Kirilova et al. [31, 32] studied CMM coatings of Zn and Co deposited in dual baths. During potentiodynamic stripping of a two-layer coating composed of a Co underlayer and a Zn overlayer [31], two separate peaks were observed; corresponding to the dissolution of both metals independently of one another. When the overlayer was of Co, the greater part of the two-layer coating was dissolved at the dissolution potential of the pure Co coatings. The authors [32] established that with increase in the number of sublayers and regardless of their individual sublayer thickness and sequence, potentials of the stripping peaks shifted positively approaching to those of pure Co coatings. Kirilova and Ivanov [33] studied the corrosion behavior of Zn–Co CMM by corrosion potential measurement and neutral salt spray (NSS) tests. In chromated CMM coatings, composed of four thick (3.0 μm) sublayers, when the oversublayer was of Zn or Co, no red rust appeared on the surface, even after 1584 h of salt spray corrosion testing. Their corrosion resistance with regard to the appearance of both white and red rust was much better than that of pure Zn or Zn–Co 0.8% alloyed coatings. Non-chromated CMM coatings, composed of 40 thin (0.3 μm) sublayers were more corrosion resistant than CMM coatings, composed of four thick (3.0 μm) sublayers having the same total thickness.

The aim of this study is to deposit smooth and bright multilayered Zn and Ni coatings, and to study their corrosion resistance by the methods of anodic dissolution of the coatings and corrosion potential measurement.

2. Experimental details

All experiments were carried out in a conventional electrochemical glass cell. The cathode was a 1 cm^2

copper (or platinum) plate and both anodes were 2 cm^2 platinum plates. The cathode surface was polished with emery paper (grit 600), degreased in an ultrasonic UM-2 bath and then etched in 1:1 HNO_3 (only the copper one). The samples, for corrosion potential determination, were deposited on a copper substrate with 4 cm^2 surface area. The cathodic potential was measured relative to a mercury sulfate reference electrode (SSE) of potential $+0.670$ V vs NHE. The temperature of the deposition of Zn sublayers was 25 ± 1 °C, and that of Ni sublayers – 50 ± 1 °C, and was kept constant with a UH-16 thermostat.

CMM coatings were deposited from the following electrolytes. The zinc electrolyte contained 75 g dm^{-3} $ZnSO_4 \cdot 7H_2O$, 22 g dm^{-3} $(NH_4)_2SO_4$, 30 g dm^{-3} H_3BO_3 and the commercial additives AZ-1 (50 cm^3 dm^{-3}) and AZ-2 (10 cm^3 dm^{-3}). The AZ-1 additive was composed of ethoxylated alcohol (with a general formula $R{-}O{-}(CH_2CH_2O)_nH$, where R is an alkyl or alkylaryl radical with 1–20 carbon atoms in the alkyl group, n is from 3 to 30 and of a Na or K salt of benzoic acid. The AZ-2 brightening additive was composed of benzylidene acetone and ethanol. The pH of the electrolyte was 4.5. The nickel electrolyte contained 258 g dm^{-3} $NiSO_4 \cdot 7H_2O$, 19 g dm^{-3} $NiCl_2 \cdot 6H_2O$, 45 g dm^{-3} H_3BO_3, 2 g dm^{-3} saccharine, 10 cm^3 dm^{-3} 30% solution of hydroxyethylated buthyn-2-diol-1,4 (EAA) and 2 mg dm^{-3} Na-decylsulfate (EFAP). The pH of the electrolyte was 2.5.

The galvanostatic deposition of Zn–Ni CMM coatings from dual baths [5, 7–13] was carried out by consecutive deposition of Zn and Ni sublayers from the electrolytes described above using a TEC 50 galvanostat. The current was measured with an ammeter (ML-10), and the potential with a digital voltmeter (V542.1). Each sublayer was deposited at a current density of 3 A dm^{-2} for different times, depending on the thickness desired. Ni sublayers of thickness 0.7 μm were deposited for 1 min and those of Zn for 45 s. Ni sublayers of thickness 3.0 μm were deposited for 5 min, and those of Zn for 3 min and 45 s. Between successive depositions the coated surfaces were rinsed with distilled water. The thickness of the sublayers was determined by measuring the amount of electricity consumed for their dissolution and using Faraday's laws.

The potentiodynamic dissolution (stripping) of the CMM coatings was carried out at 50 ± 1 °C in the Zn electrolyte without additives using a potentiostat (EP20A Elpan) and a scanner (EG20 Elpan) within the potential range -1.5 to $+0.5$ V vs SSE at a scan rate of 2 mV s^{-1}. The current–potential dependence (stripping voltammogram or curve) was recorded on a X–Y plotter (Endim 622.01).

The corrosion potentials of the coatings were measured at open circuit using a digital voltmeter (V542.1) in an electrolyte with $pH = 6$, containing 6 g dm^{-3} NaCl and 94 g dm^{-3} Na_2SO_4. The potentials were registered at a room temperature after 48 h.

3. Results and discussion

3.1. *SEM examinations*

The CMM coatings produced under the above conditions were characterized by their top layer surface appearance and surface and cross-sectional morphology which were examined on a JSM 5 300 scanning electron microscope (SEM). It was observed that the deposits either with a Ni or a Zn oversublayer were white in color and had a bright shiny silver appearance. Surface blemishes were not observed with the naked eye.

Figure 1 shows the cross-sectional morphology of a multilayered zinc–nickel coating composed of 11 sublayers beginning and ending with a Ni sublayer on a copper substrate. The specimen shows cracks between sublayers attributable to mechanical damage that occurred during the preparing of the cross-sections by metallographic techniques.

Figure 2 shows the surface morphology of the coating with a Zn oversublayer. The coating is smooth, fine-grained and without pores on the surface. The surface morphology of the coating with a Ni oversublayer was similar.

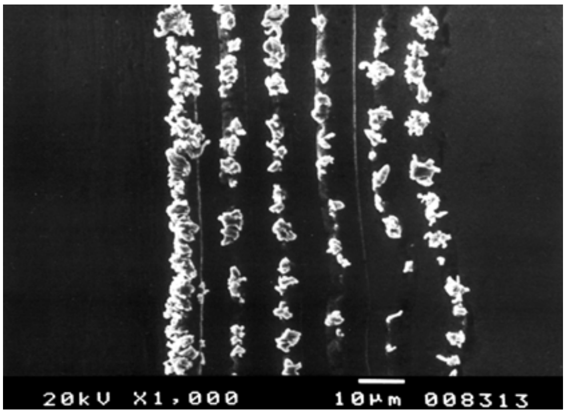

Fig. 1. Cross-sectional morphology of Zn–Ni CMM coating.

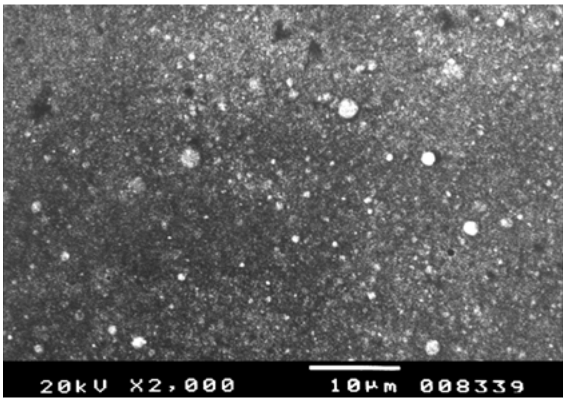

Fig. 2. Surface morphology of Zn–Ni CMM coating ending with a Zn oversublayer.

3.2. *Potentiodynamic stripping of Zn–Ni CMM coatings*

Figures 3 and 4 show stripping voltammograms of coatings with 0.7 μm individual sublayer thickness consisting of 11 (Figure 3 curve 3) and 12 (Figure 4 curve 2) sublayers with a Zn oversublayer; and of coatings consisting of 11 (Figure 3 curve 4) and 12 (Figure 4 curve 3) sublayers with a Ni oversublayer as well as of Zn coatings with thickness equal to the total thickness of five (Figure 3 curve 1) or six (Figure 3 curve 2 and Figure 4 curve 1) sublayers. On the stripping curves two separate peaks (at −1.250 V and at 0.00 to +0.100 V) are observed; corresponding to the dissolution of metals with different corrosion resistance. At more negative potential (−1.250 V) only pure Zn dissolves (Figure 3 curves 1 and 2 and Figure 4 curve 1). The stripping curves of the other studied CMM coatings with 0.7 or 3.0 μm individual sublayer thickness are similar.

By graphical integration, the area included between the axis of potential development and the whole stripping curve was determined, revealing the quantity of electricity (q, Coulombs) required for the dissolution of the whole CMM coating. Similarly, the area included between the axis of potential development and the stripping peak at more negative potential was determined, revealing the quantity of electricity (q^{I}, Coulombs) required for the dissolution of a part of the less corrosion resistant metal zinc. q^{I}/q characterizes the corrosion resistance of the CMM coatings. With decrease of q^{I}/q the corrosion resistance increases.

Figure 5 curve 1 shows the dependence of q^{I}/q on the number of sublayers for CMM coatings with 0.7 μm individual thickness ending with a Zn oversublayer. Coatings composed of an even number of sublayers begin with a nickel and end with a zinc sublayer. Coatings composed of an odd number of sublayers begin and end with a zinc sublayer. It can be seen that with increase in the number of sublayers q^{I}/q decreases from 50 to 30%. At more negative potentials (between −1.250 and −0.750 V) the zinc oversublayer and part of the zinc sublayers beneath it dissolve. After the dissolution of the Zn oversublayer, the nickel sublayers under it protect the rest of zinc sublayers and they strip together with the nickel sublayers at a substantially more positive potential (between −0.250 and +0.250 V).

Figure 5 curve 2 shows the same dependence, obtained from the stripping curves of CMM coatings ending with a Ni oversublayer. Coatings composed of an even number of sublayers begin with a zinc and end with a nickel sublayer. Coatings composed of an odd number of sublayers begin and end with a nickel sublayer. In this case, a smaller part of the zinc dissolves at more negative potentials and q^{I}/q is considerably smaller (between 20 and 25%). The q^{I}/q (curve 2) depends slightly on the number of sublayers. Results show that the nickel oversublayer protects the remaining zinc sublayers under it. As a result only a small part of the zinc dissolves through the pores of the nickel oversublayer.

In both cases the protective action increases with increase in the number of nickel sublayers because the porosity is reduced by the increasing thickness [1].

Similar dependencies are observed in CMM coatings composed of 3.0 μm thick sublayers ending with a Zn (Figure 6 curve 1) and with a Ni (Figure 6 curve 2)

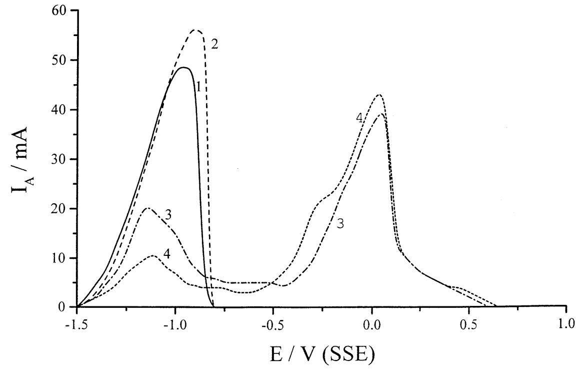

Fig. 3. Stripping voltammograms of Zn–Ni CMM coatings deposited from dual baths. (1) 3.5 μm Zn; (2) 4.2 μm Zn; (3) [0.7 μm Zn + 0.7 μm Ni]$_5$ + 0.7 μm Zn; (4) [0.7 μm Ni + 0.7 μm Zn]$_5$ + 0.7 μm Ni.

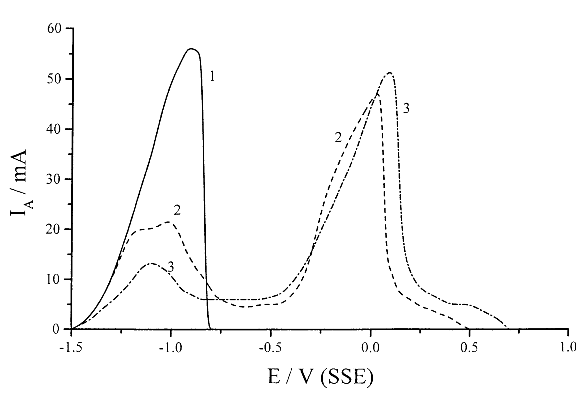

Fig. 4. Stripping voltammograms of Zn–Ni CMM coatings deposited from dual baths. (1) 4.2 μm Zn; (2) [0.7 μm Ni + 0.7 μm Zn]$_6$; (3) [0.7 μm Zn + 0.7 μm Ni]$_6$.

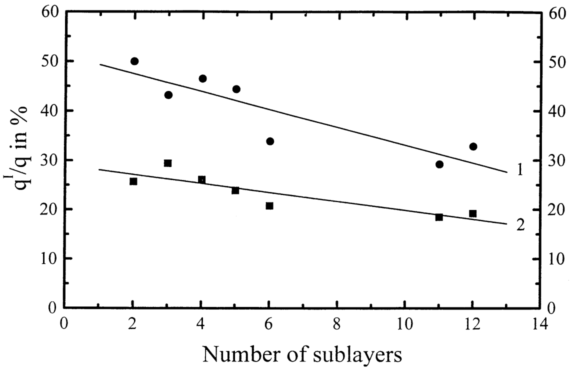

Fig. 5. Dependence of the correlation between the quantity of Zn dissolved at more negative potentials and the whole quantity of the metal in the coating (q^{I}/q) on the number of sublayers. Individual sublayer thickness 0.7 μm. (1) CMM coatings ending with a Zn oversublayer. (2) CMM coatings ending with a Ni oversublayer.

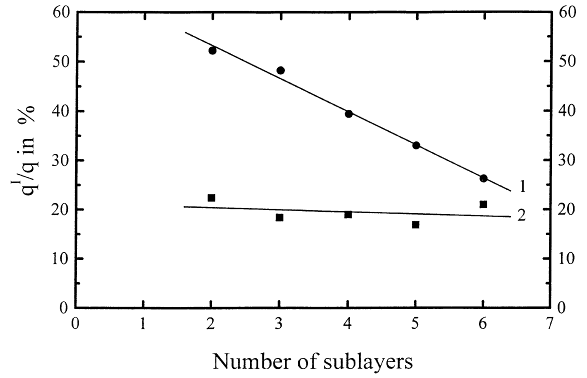

Fig. 6. Dependence of the correlation between the quantity of Zn dissolved at more negative potentials and the whole quantity of the metal in the coating (q^I/q) on the number of sublayers. Individual sublayer thickness 3.0 μm. (1) CMM coatings ending with a Zn oversublayer. (2) CMM coatings ending with a Ni oversublayer.

oversublayer. q^I/q is considerably smaller when the CMM coating ends with a Ni oversublayer (curve 2) in comparison to the case with a Zn oversublayer (curve 1). In both cases the protective effect of the thick Ni sublayers (3.0 μm) is great enough and only 20 to 25% of the CMM coating composed of six sublayers dissolves within the potential range −1.250 to −0.750 V vs SSE.

q^I/q obtained during stripping of CMM coatings composed of 11 or 12 thin (0.7 μm) sublayers (with a total thickness of 9 μm) are equal to those obtained during the stripping of CMM coatings composed of six thick (3.0 μm) sublayers (with a total thickness of 18 μm). Consequently, the CMM coatings consisting of a large number (11–12) of thin (0.7 μm) sublayers have corrosion resistance equal to those of CMM coatings consisting only of six thick (3.0 μm) sublayers.

3.3. *Definition of the corrosion potentials*

Table 1 shows the corrosion potentials of Zn and Ni coatings of thickness 7.7 or 15 μm, and of CMM coatings consisting of 11 or 12 thin (0.7 μm) sublayers and of five or six thick (3.0 μm) sublayers. It is seen that Zn coatings have the most negative potentials (between −1.405 and −1.415 V), and Ni coatings have the most positive potentials (between −0.555 and −0.570 V). CMM coatings consisting of five or six thick (3.0 μm) sublayers ending with a Zn oversublayer have corrosion potentials between −0.955 and −0.965 V. More positive are the corrosion potentials of the coatings, consisting of 11 or 12 thin (0.7 μm) sublayers with a Zn oversublayer, respectively −0.820 and −0.775 V, which are closer to that of the pure Ni coating because of the dissolution of the Zn oversublayer. The corrosion potentials of the coatings, ending with a Ni oversublayer are in the range −0.750 to −0.800 V. The corrosion potentials of CMM coatings composed of a large number of thin (0.7 μm) sublayers (with a total thickness of 8–9 μm) are equal to or more positive than the corrosion potentials of CMM coatings composed of five or six thick (3.0 μm) sublayers (with a total thickness of 18 μm). In all CMM coatings the alternation of Zn and Ni sublayers leads to an increase in corrosion resistance.

4. Conclusions

Smooth and bright Zn–Ni compositionally modulated multilayered coatings may be obtained by means of consecutive deposition of Zn from sulfate electrolyte, and of Ni from sulfate–chloride electrolyte in the presence of organic brightening additives at a current density of 3 A dm^{-2}.

With increase in the number of sublayers, regardless of their individual thickness, the correlation between the quantity of Zn, dissolved at more negative potentials (between −1.250 and −0.750 V), and the whole quantity of the metal in the CMM coatings, decreases. This correlation is smaller in CMM coatings ending with a Ni oversublayer compared to coatings ending with a Zn oversublayer.

The corrosion potentials of CMM coatings ending with a Zn oversublayer composed of 11 or 12 thin (0.7 μm) sublayers are 0.150 to 0.200 V more positive than the potentials of CMM coatings composed of five

Table 1. Values of the corrosion potentials E_{corr}/V vs SSE of Zn–Ni CMM coatings

Type of CMM	Number of sublayers	E_{corr}/V (SSE)
0.7 μm Zn	11	−1.415
[0.7 μm Zn + 0.7 μm Ni]$_5$ + 0.7 μm Zn	11	−0.820
[0.7 μm Ni + 0.7 μm Zn]$_6$	12	−0.775
3.0 μm Zn	5	−1.405
[3.0 μm Zn + 3.0 μm Ni]$_2$ + 3.0 μm Zn	5	−0.955
[3.0 μm Ni + 3.0 μm Zn]$_3$	6	−0.965
0.7 μm Ni	11	−0.555
[0.7 μm Ni + 0.7 μm Zn]$_5$ + 0.7 μm Ni	11	−0.795
[0.7 μm Zn + 0.7 μm Ni]$_6$	12	−0.750
3.0 μm Ni	5	−0.570
[3.0 μm Ni + 3.0 μm Zn]$_2$ + 3.0 μm Ni	5	−0.780
[3.0 μm Zn + 3.0 μm Ni]$_3$	6	−0.800

The coatings were deposited from dual baths after 48 h exposure in solution containing 94 g dm^{-3} Na_2SO_4 and 6 g dm^{-3} NaCl in dependence on the number, sequence and thickness of sublayers.

or six thick (3.0 μm) sublayers. The corrosion potentials of the CMM coatings ending with a Ni oversublayer are the most positive (-0.750 to -0.800 V); i.e. these multilayered coatings are the most corrosion resistant.

CMM coatings consisting of a large number of thin sublayers are more corrosion resistant than the CMM coatings consisting of a few thick sublayers with the same total thickness.

Acknowledgements

The authors wish to acknowledge financial assistance provided by the National foundation – 'Scientific Investigation' – Bulgaria.

References

1. D. Gabe, *Electochim. Acta* **39** (1994) 1115.
2. W. Blum, *Trans. Am. Electrochem. Soc.* **40** (1921) 307.
3. H. Koeppe, PhD thesis, Universitat Giessen (1923), from *J. Appl. Phys.* **60** (1986) 1374.
4. W. Deubner, *Ann. Phys.* (Leipzig) **5** (1930) 261.
5. P. Tang, P. Leisner, Per Moller, C. Nielsen and D. Nabikahni, CAG 940, 301–384.
6. J. Koehler, *Phys. Rev.* **B 2** (1970) 547.
7. J. Celis, A. Haseeb and J. Roos, *Trans. Inst. Metal Finish.* **70** (1992) 123.
8. A. Haseeb, J. Celis and J. Roos, *J. Electrochem. Soc.* **141** (1994) 230.
9. G. Wouters, M. Bratoeva, J. Celis and J. Roos, *J. Electrochem. Soc.* **141** (1994) 397.
10. G. Wouters, M. Bratoeva, J. Celis and J. Roos, *Electrochim. Acta* **40** (1995) 1439.
11. G. Barral and S. Maximovitch, *Colloque de physique C4* **51** (1990) 291.
12. L. Goldman, B. Blanpain and F. Spaepen, *J. Appl. Phys.* **40** (1986) 1374.
13. C. Ross, L. Goldman and F. Spaepen, *J. Electrochem. Soc.* **140** (1993) 91.
14. M. Kalantary, G. Wilcox and D. Gabe, *Brit. Corr. J.* **33** (1998) 197.
15. G. Chawa, G. Wilcox and D. Gabe, *Trans. Inst. Metal. Finish* **76** (1998) 117.
16. R. Steigerwand and N. Green, *J. Electrochem. Soc.* **109** (1962) 1026.
17. S. Swathirajan, *J. Electrochem. Soc.* **133** (1986) 671.
18. V. Jovic, R. Zejnilovic, A. Despic and J. Stevanovic, *J. Appl. Electrochem.* **18** (1988) 511.
19. S. Swathirajan, *J. Electroanal. Chem.* **221** (1987) 211.
20. P. Andricacos, J. Tabib and L. Romankiw, *J. Electrochem. Soc.* **135** (1988) 1172.
21. P. Andricacos, C. Avana, J. Tabib, J. Dukovic and L. Romankiw, *J. Electrochem. Soc.* **136** (1989) 1336.
22. K. Wong and P. Andricacos, *J. Electrochem. Soc.* **137** (1990) 1087.
23. J. Horkans, I-C. Hsu Chang, P. Andricacos and E. Podlaha, *J. Electrochem. Soc.* **138** (1991) 411.
24. V. Jovic, A. Despic, J. Stevanovic and S. Spaic, *Electrochim. Acta* **34** (1989) 1093.
25. V. Jovic, S. Spaic, A. Despic, J. Stevanovic and M. Pristavic, *Mater. Sci. Technol.* **7** (1991) 1021.
26. L. Skibina, J. Stevanovic and A. Despic, *J. Electroanal. Chem.* **310** (1991) 391.
27. J. Stevanovic, I. Kovrigina and A. Despic, *J. Serb. Chem. Soc.* **56** (1991) 217.
28. J. Stevanovic, V. Jovic and A. Despic, *J. Electroanal. Chem.* **349** (1993) 365.
29. V. Jovic, B. Jovic and A. Despic, *J. Electroanal. Chem.* **357** (1993) 357.
30. V. Jovic and V. Jevtic, *J. Serb. Chem. Soc.* **61** (1996) 479.
31. I. Kirilova, I. Ivanov and St. Rashkov, *J. Appl. Electrochem.* **28** (1998) 637.
32. I. Kirilova, I. Ivanov and St. Rashkov, *J. Appl. Electrochem.* **28** (1998) 1359.
33. I. Kirilova and I. Ivanov, *J. Appl. Electrochem.* **29** (1999) 1133.